Biogenic Synthesis Of Copper Nanoparticles Using Ficus Religiosa Leaves Extract (Fcu Nps) And Assessment Of Their Antimicrobial And Antibiofilm Potential Against Wound-Associated Biofilm-Forming Pathogens.

S. Chaudhary [1*], A. Jyoti [2], V. Shrivastava[3*] and R. S. Tomar[4]
Amity Institute of Biotechnology, Amity University Madhya Pradesh, Gwalior, Maharjpura Dang, Gwalior-474005, India

[*]Corresponding author- vshrivastava@gwa.amity.edu
Mail ID – suruchichaudhary02@gmail.com

Abstract:

This study is related to the biosynthesis of copper nanoparticles using plant extracts of Ficus religiosa (peepal vriksh) and its potential as an effective antimicrobial agent, with special reference to wound-associated pathogens that are reported to form biofilms in chronic wounds. Wound biofilm-forming microorganisms hinder the healing process, and the clinical samples taken from wounds were processed. The identification and pathogenicity of the isolated microbes were tested using biochemical and hemolysis tests. The biosynthesis of copper nanoparticles was performed using Ficus religiosa plant leaf extract and was characterized using UV-visible, XRD, and FTIR techniques, and their efficacy was evaluated using the well-diffusion method. According to the observed hemolytic patterns, the microbes isolated from the wound samples were pathogenic. The synthesized copper nanoparticles had an average size of 26–100 nm. These materials are eco-friendly, economical, and biocompatible. The synthesized particles have shown effective antimicrobial and antibiofilm properties against wound-associated pathogens; thus, they can be used for drug design purposes to sustain the fast healing of chronic wounds infected with biofilm-forming pathogens.

Key words: Biofilm, Wound Biofilm, Anti-biofilm, Nanotechnology, Anti-oxidant, Copper Nanoparticles.

Introduction

'Biofilm' is a term given by Wilderer and Charaklis in 1989 to depict the comparatively ineffable microbial summation that is allied with a surface or some other substantial non-flicking material, conjecturally dispensed in a framed matrix or glycocalyx.[1] Biofilm is a complex microbial community created by planktonic or sessile microorganisms that can be rapidly expressed by secreting extra polymeric substances and 80 new proteins.[2, 3] Biofilm grows within 1 or 2 hours of attachment from a small single colony to a complex microbial community. Biofilms have their

own defence systems due to the presence of multiple colonies of microorganisms, which provide complexity as well as resistance against biocides, antibiotics, and the host immune system.[4]

The microflora located in the wound site is commonly referred to as the wound microbiota" or wound microbiome, which can be defined as “whole microorganisms that are found on or in the site of the wound and its proximate expansion”.[5] Ongoing investigations have shown that polymicrobial communal colonies present in the wound microbiome are responsible for the formation of complex biofilms, impairing the host’s immune responses and healing processes, leading to delayed healing.[6] Due to high inflammation at the site of the wound, bioburden increases and creates a major problem in the healing process as it constitutes descendent tissue cells, proteinaceous exudates, and microorganisms.[7] And biofilms are impervious to the host immune system and can flourish on secreted exudates and promote inflammation.[8,9,10]

In any person’s lifetime, on multiple occasions, wounds may occur as a result of an injury or accident. When the dermal layer of the skin is damaged and becomes open to the environment, it results in an open wound. Nearly one billion people worldwide suffer from acute and/or chronic wounds.[11]

According to James et. al., in wounds, biofilm formation exhibits only in 60% of chronic wounds whereas in acute wounds only 6% of biofilm is incorporated i.e., acute wounds have traces of biofilm while in chronic wounds its complex and well flourished. Generally, acute wounds heal within 2-4 weeks while deep chronic wounds can take up to 4-6 months in the same area An acute wound microbiome shows fewer microbes i.e., 4-5 log reduction viability, whereas in chronic wounds 2-3 log reduction viability phases.[4] If sessile microbes evade the immune system of the host and are allowed to establish a biofilm, then it turns an acute wound into a chronic state in a short time.

Because of the developed resistance system towards available antibiotics and biocides, it is difficult to eradicate a biofilm infection in a short period of time, which increases the chronicity of the wound and ultimately leads to delayed healing.[12,13,14]

Nanotechnology is a fast-growing branch of science because of its various potential applications in various fields, such as medicine, healthcare, agriculture, and engineering. Nanoparticles (NPs) and nanomaterials have been used globally for various purposes. They can be synthesized using physical, chemical, and biological methods. However, nanoparticles and nanomaterials synthesized via the green route method, that is, biological methods, are the most promising and easily acceptable in the medical field as they are eco-friendly, safer, more biocompatible, more

effective, and non-toxic to certain limits.[15,16,17]

2 Material and methods

2.1 Isolation, biochemical and pathogenicity identification of wound-associated pathogens

Clinical samples were collected from deep/chronic wounds that were suspected to have a recurrent infection or in which biofilm-forming pathogens may be present. All clinical samples were obtained after obtaining consent and anonymized prior to testing. Samples were processed using the spread plate and streak plate methods to obtain single culture colonies, which were further identified as pure cultures by performing different biochemical tests. The isolated microorganisms were further tested to determine their pathogenic potential using a hemolysis test. All strains isolated from the clinical samples were streaked on sheep blood agar plates containing 5% defibrinated sheep blood.[18].

2.2 Biofilm Formation:

2.2.1 Congo Red Agar Test

The Congo Red Agar method was used to check the biofilm-forming ability of microbes. This test is based on subculturing of the test microorganism on Brain Heart Infusion Agar (BHI) supplemented with sucrose sugar and Congo dye.[19] It is one of the easiest and most inexpensive methods for detecting biofilm-forming microorganisms. This method was modified to obtain sharp results [20] as the percentage of components that were added or substituted per requirement. (Figure 3)

2.2.2 Microtiter Plate Method

The crystal-violet assay was performed to detect biofilm formation. Sterile 150 microliters of tryptone soy broth were added to the 96-well microtiter plate. 50 microliters of overnight bacterial cultures of the isolated samples were added to the desired wells and incubated for 48 hours in a shaker incubator at 120 rpm at 37°C. After the first incubation, the wells were decanted and filled with fresh TS broth and incubated further for 24 hours in a shaker incubator at 120 rpm at 37°C. After the second incubation, the plate was decanted and air-dried. The dried wells were washed with normal saline twice, stained using 0.4% crystal-violet dye, and left on the plate for 15-20 minutes. Once the resting period was over the wells were washed with distilled water and filled

with 33% glacial acetic acid. The absorbance was taken at 600nm using a microtiter plate reader [21, 22]. Biofilm formed or not can be confirmed by referring to Table 1 [23].

Table 1 Showing reference readings for Biofilm formation

Sr. No.	**Absorbance**	**Bacterial Adherence**	**Biofilm Formed**
1.	<0.120	None	None/Weak
2.	0.120-0.240	Moderate	Moderate
3.	≥0.240	Strong	High

Alternatively, biofilm can be calculated using a formula that tells us about specific biofilm formation. Details are given in Table 2 [24] below.

Table 2 Showing Reference Formulae for calculating Biofilm formation

Sr. No.	**Formula**	**Strong(S)**	**Moderate(M)**	**Weak(W)**	**Negative (N)**
1.	BF = AB - CW	≥0.300	0.200-0.299	0.100-0.199	<0.100
2.	BF = AB⁄CW	≥6.00	4.00-5.99	2.00-3.99	<2.00
3.	SBF = (AB - CW)⁄G	≥1.10	0.70-1.09	0.35-0.69	<0.35

2.3 Collection of Plant leaves and plant extract preparation

Fresh leaves of the selected plant "Ficus religiosa" were collected from the area of Morar cant., Gwalior, and the botanical garden of Jiwaji University, Gwalior. Healthy leaves were sorted, washed, and air-dried. Sorted leaves (20 g) were ground in a mortar and pestle with distilled water, and the obtained slurry was kept in 50% ethanol for 12-24 hours with constant agitation. The slurry was further filtered twice with a muslin cloth to remove any undesired parts and with Whatman's filter paper no. 1. The filtrate was stored at 4 °C.

2.3 Phytochemical analysis

2.3.1 Qualitative Analysis

To confirm the presence of different phytochemicals, fresh leaf extracts of Ficus religiosa were subjected to different qualitative tests, which confirmed the presence of alkaloids, glycosides, flavonoids, tannins, phenolics, saponins, terpenoids, steroids, catechins, coumarins, quinones, and xanthoproteins. [25]

2.3.2 Quantitative Analysis (HPLC)

HPLC is an adaptable, vigorous, and novel strategy utilized in phytochemical and scientific science to distinguish, measure, and clean the singular parts of any combination. This unique investigation technology shows only the similarity results calculated based on the relative value, that is retention time, with the selected marker compound as a reference standard. [26]

2.3.3 Antioxidant Activity of Ficus religiosa leaves extract (DPPH radical scavenging activity)

The radical scavenging of the plant extract was done using DPPH (1,1 diphenyl 2-picryl hydrazyl). [27] Antioxidants present in the leaves extract reduces DPPH to DPPH-H resulting in a decrease of absorbance. 0.1nM DPPH solution was prepared by dissolving 4mg of DPPH in 100 mL ethanol. Ascorbic acid 10mg/mL was used as a reference. Different volumes of plant extract made up with DMSO and 2.96ml of DPPH. The reaction mixture was incubated in dark conditions for 20 minutes. The absorbance of the mixture was recorded at 517 nm.

2.4 Biological Synthesis of copper nanoparticles and their characterization

0.1 M solution of copper II sulfate pentahydrate was placed in an Erlenmeyer flask and stirred continuously on a magnetic stirrer for 2–3 h at room temperature. For the purpose of reduction, the ethanolic leaf extract of *Ficus religiosa* was added dropwise at intervals of 30-40 minutes. Subsequently, the solution was dried in an oven at 60^{o}C. The obtained particles were then washed with 100% ethanol and dried. The processed particles were further characterized to study their shape, size, and other properties using techniques such as FTIR and PXRD. [28,29] (Figure 1)

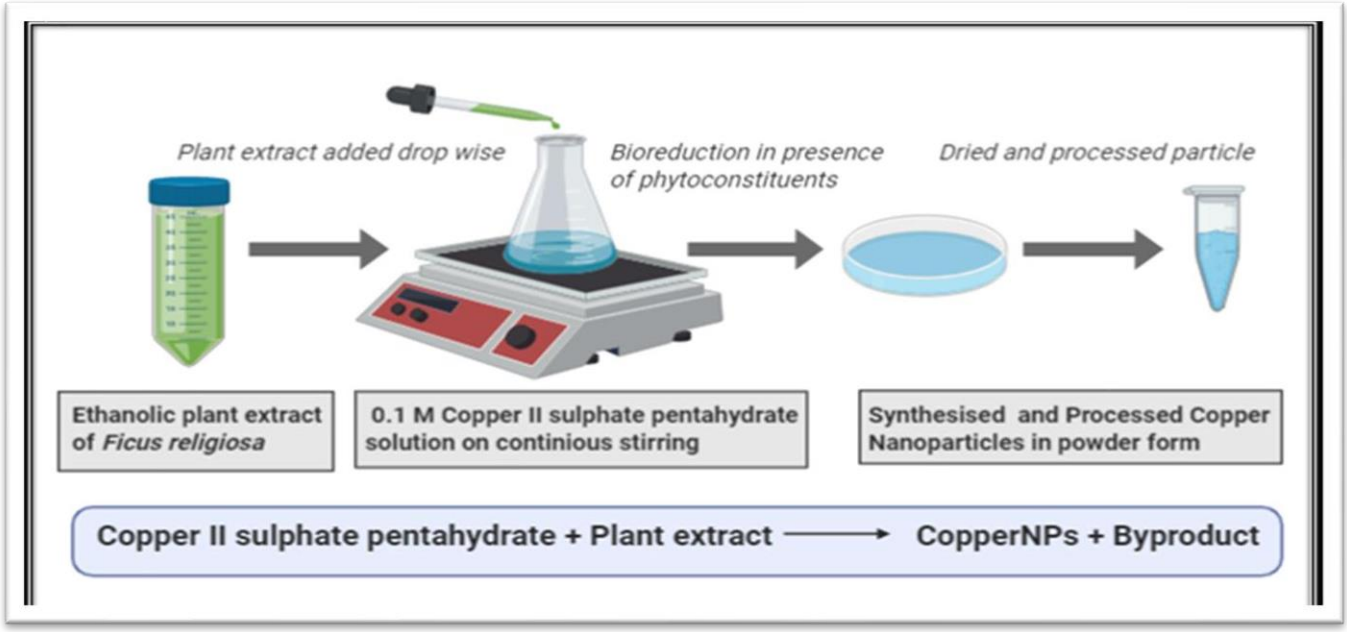

Figure 1: Biosynthesis of copper nanoparticles.

2.5 Characterization of Nanoparticles

2.5.1 Powder X-ray diffraction

To obtain information like phase composition to crystallite size, lattice structure and crystallographic orientation powdered XRD was used. This technique uses a search/match procedure to identify the components in a sample. [30,31]

Accurate quantification of the obtained experimental results for the determination of crystal structures and the average size of the crystallites was calculated using Bragg's law and Scherrer's formula.

2.5.2 Fourier Transform Infrared Spectroscopy

The FTIR analysis method uses infrared light to scan the test samples and observe the chemical properties. So, this technique was used in order to identify the presence of organic functional groups attached to the synthesised nanoparticles.

2.6 Antimicrobial Susceptibility Testing

2.6.1 Well Diffusion Method

The antimicrobial activity of synthesised copper nanoparticles was evaluated by taking the measurement of the inhibition zone produced by the particles diffused through wells created in Muller Hinton agar plates as per standard protocol. For antimicrobial Susceptibility Test: Fresh-grown pure cultures of obtained pathogenic bacteria were suspended in sterile saline. This

suspension was spread on Muller Hinton agar (MHA) plate's surface. 1mg/ml concentrations of nanoparticles were used as the final concentration of which 100 microliters were loaded in each well. The plates were kept for incubation at 37℃ for 24 hr. After the required incubation, obtained inhibition zones were measured and compared with standards. [32,33,34,35,36]

2.6.2 Antibiofilm Activity

The antibiofilm assay was performed similarly to the biofilm assay on a 96-wells microtiter plate with some changes. For antibiofilm assay 50µl overnight culture broth was taken and 150 µl fresh LB was added to wells. We incubated it on the shaker at 120rpm at 370C for 48 hours. After incubation time, we replaced the culture broth in wells with fresh autoclaved LB and again incubated the microtiter plate on a shaker at 120rpm and 37oC for 24 hours. For antibiofilm assay after incubation of 48 hours the culture broth was replaced by 100 µl of synthesized nanoparticles (1mg/ml stock solution) and the plate was again incubated for 24 hours at 370C on a shaker at 120rpm. For biofilm disruption assay, time was given to bacteria to form biofilm completely i.e. after 48 hours' culture broth in wells was replaced with fresh autoclaved LB and again microtiter plate was incubated on a shaker at 120rpm and 37oC for 24 hours. After this time bimetallic nanoparticles are added to wells and the plate was again incubated under the same conditions. Staining for antibiofilm and biofilm was done similarly as in the case of biofilm with the only difference is a biofilm and antibiofilm staining is done after 3 days of total incubation time but biofilm disruption staining is done after 4 days of total incubation time to allow biofilm to fully furnish and then the efficacy of our particles was checked. The percentage of biofilm-inhibited/ disrupted or formation percentage was calculated by applying the following formula [37, 38].

$$\% \text{ of Biofilm inhibited/disrupted} = \left[1 - \frac{\text{O.D.600 of cells treated with nanoparticle}}{\text{O.D.600 of untreated cells}}\right] \times 100$$

$$\% \text{ Biofilm growth} = 100 \times (\text{Sample}_{A600} - \text{Sterile Control}_{A600}) / (\text{Growth Control}_{A600} - \text{Sterility Control}_{A600}).$$

3 Results and Discussion

3.1 Microbiological Analysis

This analysis shows that the pus samples constitute a wide range of microorganisms, but the most prevalent and frequently isolated bacteria were SIA and SIIB to *Proteus*, SIIA to *Neisseria*, SIIIC1 to *Pseudomonas*, SIIIC2a to *Corynebacterium*, SVIIB and SIXA to *Escherichia*, SXIIB to *Klebsiella* and SXIIIC to *Staphylococcus*. Genus's identification of this pure culture required to use of a variety of biochemical tests. The dichotomous keys, "Bergey's manual of systematic bacteriology and information", accrued from previously performed laboratory procedures helped to identify the unknown genus of the obtained cultures. (Table 1.1) All the clinical isolates grew well/ effectively on sheep blood agar media. They were reported to be pathogenic according to the obtained patterns of hemolysis (alpha, beta, gamma). (Figure 2)

Table 3 Results of all Bio-chemical Tests

Sr. no.	Sample Code	Carbohydrate Fermentation Test		Indole Test	MR Test	VP Test	Citrate Test	Catalase Test	Urease Test	Nitrate Test	H2S Test	Predicted Genus
		Lactose	Glucose									
i.	SIA	-	+	-	+	-	+	+	-	+	+	*Proteus*
ii.	SIIA	-	+	-	+	-	+	+	-	-	-	*Neisseria*
iii.	SIIB	-	+	-	+	-	+	+	-	+	+	*Proteus*
iv.	SIIIC1	-	-	-	-	-	+	+	-	+	-	*Pseudomonas*
v.	SIIIC2a	-	+	-	+	-	-	+	-	+	+	*Corynebacterium*
vi.	SVIIB	+	+	+	+	-	-	+	-	+	-	*Escherichia*
vii.	SIXA	+	+	+	+	-	-	+	-	+	-	*Escherichia*
viii.	SXIIB	+	+	-	-	+	+	+	+	+	-	*Klebsiella*
ix.	SXIIIC	+	+	-	+	+	+	+	+	+	-	*Staphylococcus*

Figure 2: Haemolysis test showing different patterns of α, β, and γ haemolysis.

3.2 Biofilm Forming Microorganisms detection test

3.2.1 Congo Red Agar Test

The evaluation criteria for this method are Visual Analysis. The inoculated microorganisms form black coloured colonies which can be brown to black. The microorganisms forming brown to black colour colonies tend to form biofilm while the other colourful or colourless colonies that grow on the agar plate were said to be negative for biofilm formation. [32,33] The selected pathogenic cultures were found to be positive for the test.

Figure 3: Congo Red Agar test showing positives (Black colonies) and negatives (No colour change in colonies).

3.2.2 Microtiter Plate Method

The selected biofilm-forming pathogens were further tested with the microtiter plate method using Crystal-violet assay for their biofilm-forming ability in terms of weak, moderate and strong using this method. The readings obtained with a microtiter plate reader were calculated using the given formulae. The results have described in table 4.

Table 4: Shows the outcomes of biofilm formation in terms of the strength of the biofilm.

SR. NO.	SAMPLE CODE	OUTCOME
1.	SIA	STRONG
2.	SIIA	STRONG
3.	SIIB	STRONG
4.	SIIIC1	MORDRATE
5.	SIIIC2a	MORDRATE
6.	SVIIB	STRONG
7.	SIXA	STRONG
8.	SXIIB	MODERATE
9.	SXIIIC	MORDRATE

3.3 Collection of Plant leaves and plant extract preparation

The plant extract prepared was greenish-yellow in colour (Figure 4).

Figure 4: Plant Leaves and Plant Extract *of Ficus religiosa*.

3.4 Phytochemical analysis

3.4.1 Qualitative Analysis

The presence of bioactive compounds found in the green leaves extract of *Ficus religiosa* are Alkaloids, Glycosides, flavonoids, Tannins, phenolics, saponins, terpenoids, steroids, and coumarins. Their presence is shown in the table below where '+++' represents strong presence, '++', '+' moderate, '-' poor or not present (Table 4).

Table 4: Showing the Phytochemical analysis data with "+" (positive sign) showing the presence and "–"(negative sign) showing the absence of the phytocompounds.

Sr. No.	Biologically active Phytocompounds	*Ficus religiosa*
1.	Alkaloids	++
2.	Glycosides	+++
3.	Flavonoids	+
4.	Tannins	+++
5.	Phenolics	++
6.	Saponin	+
7.	Terpenoids	+++
8.	Steroids	++
9.	Catechins	-
10.	Coumarins	+
11.	Quinones	-
12.	Sterols	+
13.	Triterpenes	+
14.	Anthraquinones	-
15.	Xanthoproteins	-

3.4.2 Quantitative analysis (HPLC)

The presence of bioactive compounds such as gallic acid, ellagic acid, eugenol, and quercetin was confirmed and quantified by HPLC. The peaks in the chromatogram were identification was based on the retention time of the sample analyte which was separately injected and the addition of the standard analyte. According to the chromatogram (Figure 5), peak 1 is gallic acid, peak 7 is ellagic acid, peak 3 is eugenol, and peak 4 is quercetin. Quercetin, ellagic acid, eugenol, and gallic acid amounts have been determined using the standard formula and the amount found to be 10.5µg/mL, 3.89µg/mL, 4.35µg/mL, and 1.17µg/mL respectively, using the formula. The ethanolic peepal leaf extract has been found to contain the highest concentration of phenol gallic acid.

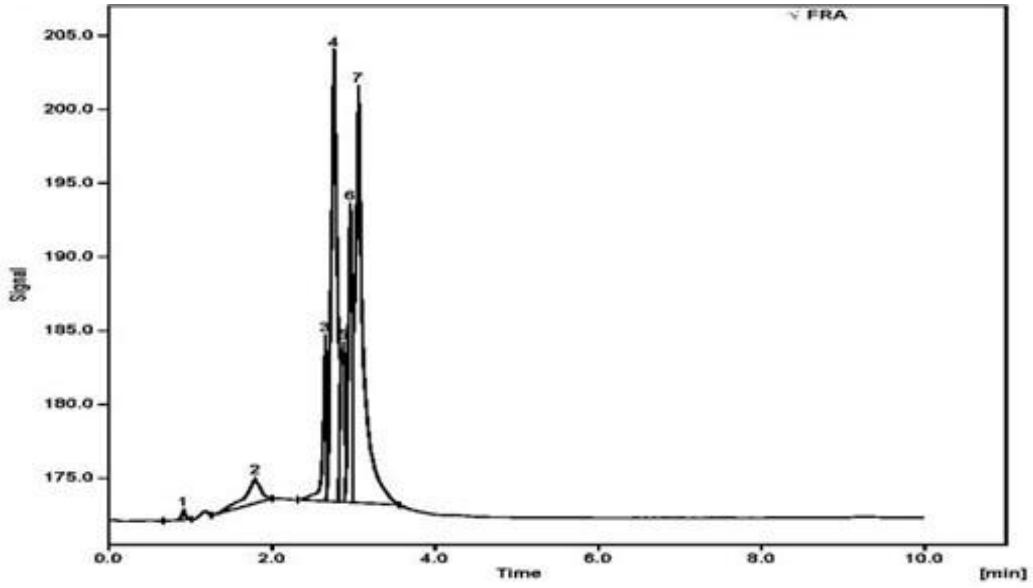

Figure 5: HPLC Graph of Ficus religiosa leaves extract showing the presence of different phytochemicals.

3.4.3 Antioxidant Activity of *Ficus religiosa* leaves extract (DPPH radical scavenging activity)

The radical scavenging activity percentage of the plant leaf extract was calculated using the below formula

$$\% \text{ radical scavenging activity} = \left[\frac{(\text{Absorbance control} - \text{Absorbance sample})}{\text{Absorbance control}} \right] \times 100$$

Where,

Absorbance control = Total radical activity without inhibitor (DPPH + Ethanol)

Absorbance sample = Activity in the presence of the test compound (DPPH + Plant extract)

Table 5: Percentage inhibition activity of *Ficus religiosa* plant extracts with ascorbic acid as standard.

Sr. no.	Concentration in µL	% inhibition by Ascorbic acid	% inhibition by *Ficus religiosa*
1.	20	68.19	61.2
2.	40	88.10	66
3.	60	93.00	66
4.	80	95.12	55
5.	100	98.33	68.8
6.	200	99.00	76.4

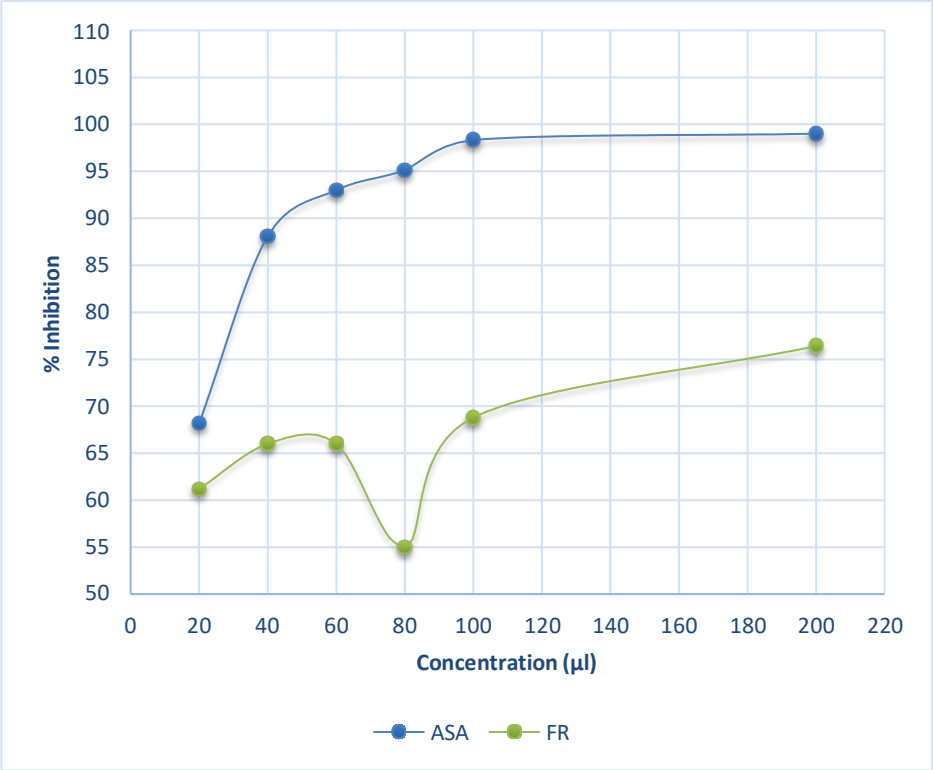

Figure 6 % inhibition of ascorbic acid standard and *Ficus religiosa* leaves extract.

3.5 Green Synthesis and Characterization of Copper Nanoparticles

3.5.1 Synthesis of FCu NPs

Synthesized Copper nanoparticles from Ficus religiosa leaves extract via biological route crystalline, and free from impurities.

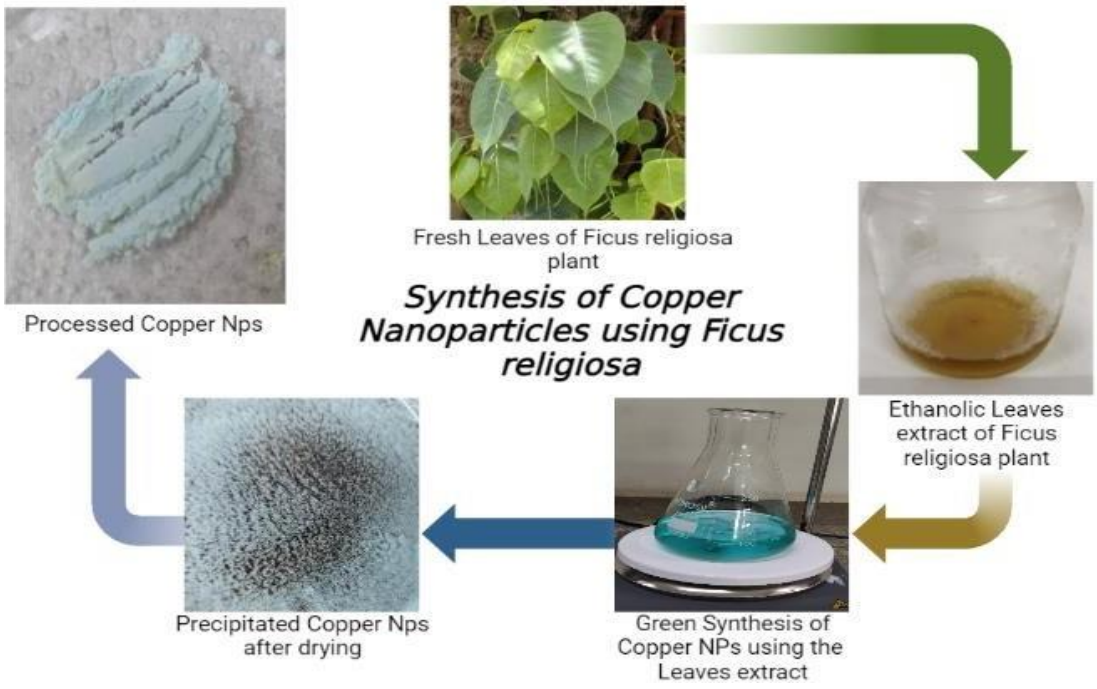

Figure 7 Shows the results of the Green synthesis of FCu NPs using *Ficus religiosa* leaves extract.

3.5.2 Characterization Synthesised Nanoparticles

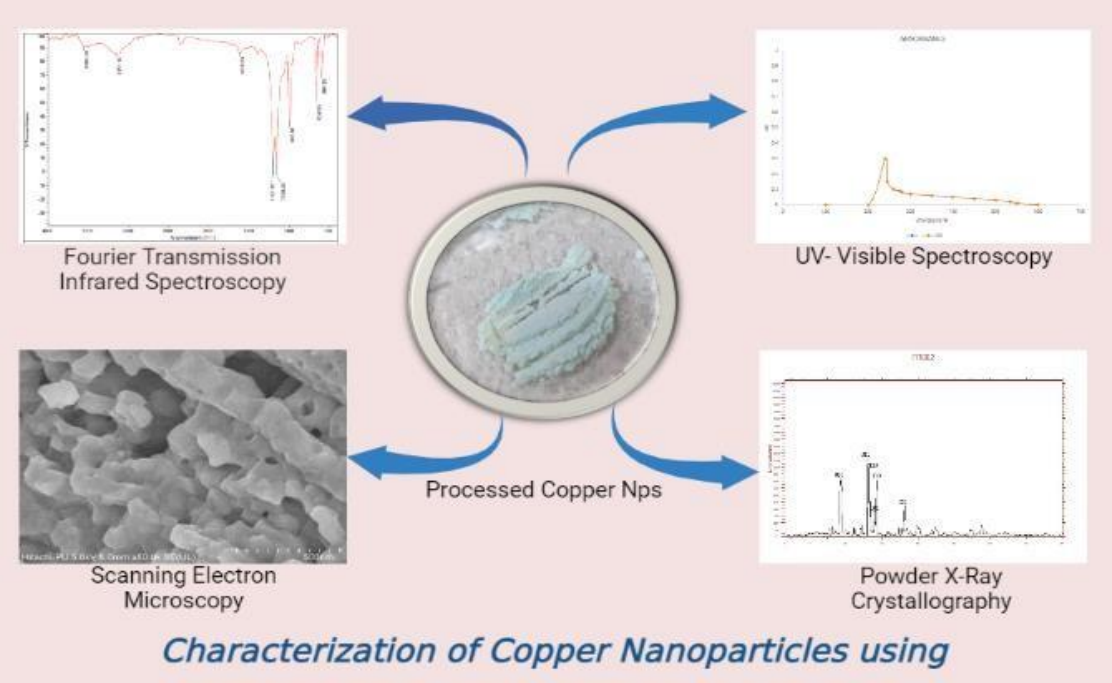

Figure 8 shows the summary of the characterization of FCu NPs.

3.5.2.1 PXRD analysis

The XRD pattern of the prepared copper nanoparticles is shown in the graph below. According to the recorded peaks with 2-theta values of 18.669, 26.496, 26.043, 27.963, 28.505, 36. 350 which are correspondent to the Miller indices (hkl) values were indexed to (100), (010), (001), (101), (110) and (111) crystallographic planes of face-centred cubic of JCPDS, File No. 04-0836. The planes may be equivalent because of symmetry in a cubic crystal, (100) (010) and (001) are equivalent. They are the family of planes (100) in Miller indices (hkl) values (figure 7). The average crystallite sizes of copper oxide nanoparticles were calculated using the "Debye-Scherrer's' equation" commonly used to calculate a relationship between peak broadening in XRD and the average size of the particle by the given equation:

$$d = k\lambda/(\beta * \cos\theta)$$

Where,

'd' is the 'particle size' of the crystal.

k is Scherrer's constant (0.9).

λ is the X-ray wavelength (0.15406 nm).

β is the width of the peak at half-height.

θ is Bragg's angle.

The given equation is used to determine the crystallite size of synthesised copper nanoparticles. The average crystallite size of the sample is in the range of 25.5 nm and the crystal lattice was Chalcanthite, tridinic and primitive type.

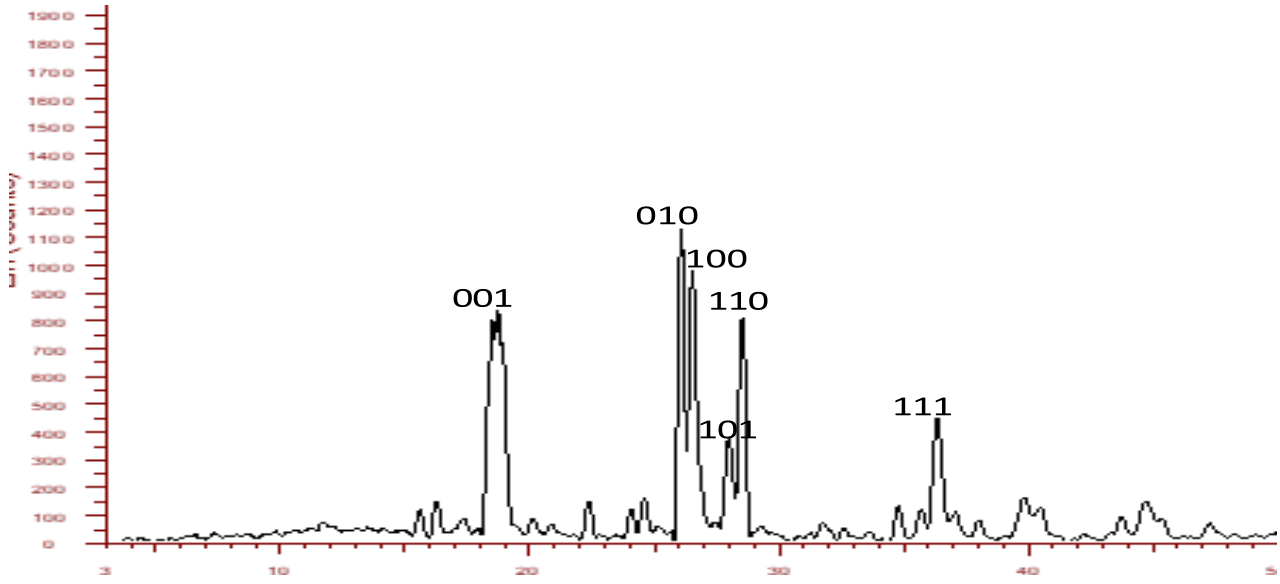

Figure 9 Graph showing PXRD data and the JCPDS no. of Copper Oxide Nanoparticles.

3.5.2.2 FTIR analysis

The FTIR analysis was performed to identify the functional group attached to the synthesised nanoparticles. It depicted that the bulk copper was reduced to nano-size particles by the phytochemicals present in the green leaves extract of Ficus religiosa. According to the table and FTIR spectra (figure 6) the band at 3553.20, 3151.14, 1615.50, 1197.85, 1156.85, 995.88, 659.95, 594.55 wavenumbers/ group frequency are corresponding to carboxylic acid (usually centred), alcohol (intramolecular bond), α- β unsaturated ketone, Tertiary alcohol, Alkene (monosubstituted), Halo Compound respectively. (Table 2)

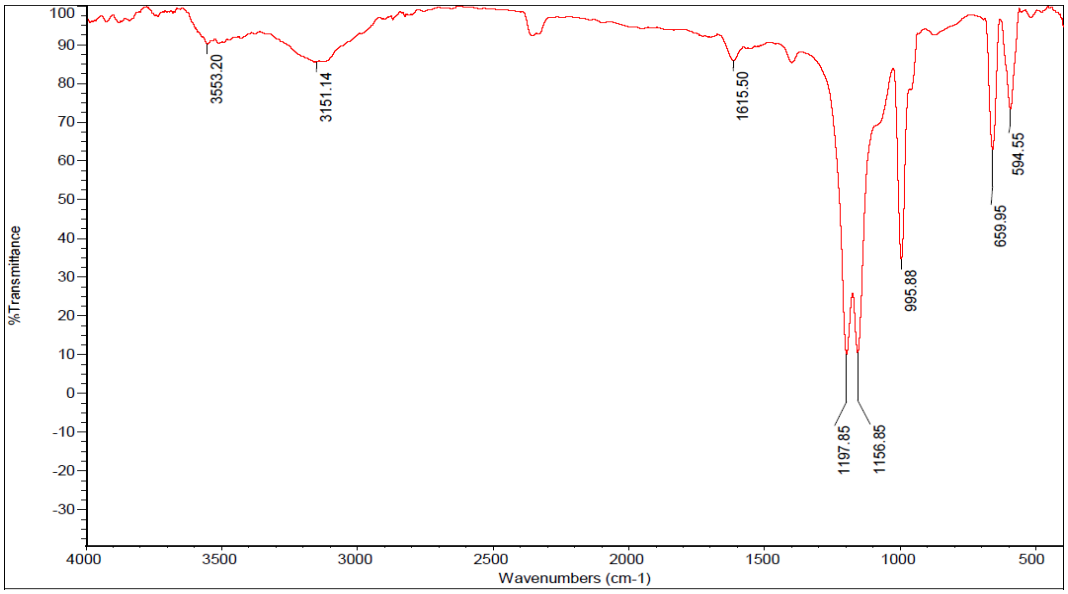

Figure 10 FTIR plot showing wavenumbers of attached functional groups.

Table 6: Showing the FTIR analysis data with group frequency, bond type, its origin and the attached functional group.

Sr. No.	Wavenumber Or Group Frequency (Cm^{-1})	Bond Type	Bond Origin	Functional Group
1.	3553.20 to 3151.14	Strong, Weak	Broad O-H Stretching	Carboxylic acid (usually centred), alcohol (intramolecular bond)
2.	1615.50	Strong	C=C Stretching	α- β unsaturated ketone
3.	1197.85	Strong	C-O Stretching	Tertiary alcohol
4.	1156.85	Strong	C-O Stretching	Tertiary alcohol
5.	995.88	Strong	C=C Bending	Alkene (monosubstituted)

6.	**659.95**	**Strong**	**C-Br Stretching**	**Halo Compound**
7.	**594.55**	**Strong**	**C-Br/I Stretching**	**Halo Compound**

3.6 Antimicrobial Susceptibility Testing

Pelletier et al., 2010, suggested that the reactivity of different nanoparticles against microbes is highly dependent on the morphology and the surface mass ratio. All the particles have different binding characteristics with the microbial surface due to their biological and chemical reactive edges and corners. The antibacterial potential of the synthesised copper nanoparticles against the clinically isolated pathogenic strains was tested and based on the observed zone of inhibition they were found to be effective (table 3). The observed results had shown an effective bactericidal activity at 1mg/ml nanoparticle concentration in 100µL nanofluid in each well (figure 8).

Table 7: Showing the Antimicrobial Susceptibility Results

Sr. No.	**Culture Number**	**Observed zone of inhibition (in mm) on different concentrations of nanoparticles.**			
		Control (Drug)	**Average ZOI**	**SD**	**SE**
1.	**SIA**	**10**	**29**	**±4.00**	**±2.30**
2.	**SIIA**	**10**	**23**	**±5.03**	**±2.90**
3.	**SIIB**	**NIL**	**19**	**±1.00**	**±0.57**
4.	**SIIIC1**	**NIL**	**21**	**±1.00**	**±0.57**
5.	**SIIIC2a**	**NIL**	**17**	**±2.08**	**±1.20**
6.	**SVIIB**	**12**	**16**	**±2.65**	**±1.53**
7.	**SIXA**	**14**	**25**	**±3.00**	**±1.73**
8.	**SXIIB**	**12**	**15**	**±2.52**	**±1.45**
9.	**SXIIIC**	**10**	**36**	**±2.08**	**±1.20**

Figure 11: Antimicrobial Susceptibility test showing Zones of Inhibitions resulting from the effect of Copper Nanoparticles

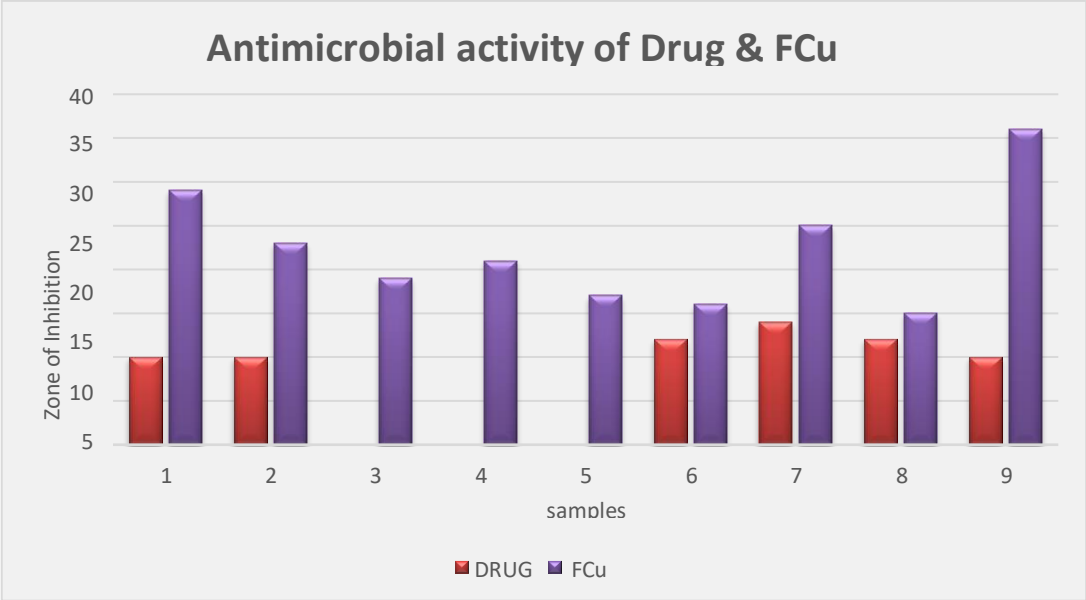

Figure 12: Graphical Representation of Antimicrobial Susceptibility test showing that the FCuNPs worked well as antimicrobial agents over the conventional drug.

3.7 Antibiofilm Activity

The synthesized metallic nanoparticles have shown significant antibiofilm and biofilm disruption activity against all the clinical isolates. The particles may have interfered with the adhesion and EPS formation capability of biofilm-forming bacteria resulting in no formation and disruption of the formed biofilm. The results shown in Table 8 are the readings obtained after staining the treated wells for inhibition (antibiofilm) and biofilm disruption. Tables 9 and 11 have shown the inhibition and disruption percentages of the treated wells. Biofilm growth percentages with and after the treatment of nanoparticles and drug alone and synergistically are shown in Tables 10 and 12

Table 8: Readings of Anti-Biofilm and Inhibition Activity Assay of FCu NPs alone and Synergistic with Antibiotic at 600nm (Au cm^{-1})

Antibiofilm (Inhibition and Disruption) Activity of FCu Nanoparticles								
CULTURE CODE	**PC**	**DRUG (I)**	**FROO2 (I)**	**FROO2+ DRUG (I)**	**DRUG (D)**	**FROO2 (D)**	**FROO2+ DRUG (D)**	**BLANK**
C1 (SIA)	**2.0057**	**0.0016**	**0.0130**	**0.0424**	**0.0549**	**0.0161**	**0.0300**	**0.0807**
C2 (SIIA)	**2.2803**	**0.1469**	**0.1532**	**0.2504**	**0.1371**	**0.0249**	**0.1408**	**0.0790**
C3 (SIIB)	**0.875**	**0.0013**	**0.0228**	**0.0354**	**0.0526**	**0.0303**	**0.0311**	**0.0813**
C4 (SIIIC1)	**2.8446**	**0.0973**	**0.0250**	**0.0184**	**0.0120**	**0.0522**	**0.2657**	**0.1416**
C5 (SIIIC2a)	**2.0228**	**0.1802**	**0.0041**	**0.0376**	**0.0112**	**0.0040**	**0.0534**	**0.0788**
C6 (SVIIB)	**1.2945**	**0.0417**	**0.0494**	**0.0509**	**0.0518**	**0.0527**	**0.0465**	**0.0867**
C7 (SIXA)	**1.6386**	**0.0467**	**0.0293**	**0.0102**	**0.0484**	**0.0195**	**0.0330**	**0.0846**
C8 (SXIIB)	**1.846**	**0.0087**	**0.0947**	**0.0268**	**0.0509**	**0.0043**	**0.0176**	**0.0839**
C9 (SXIIIC)	**2.6141**	**0.0358**	**0.1035**	**0.0463**	**0.0472**	**0.0113**	**0.0148**	**0.0797**

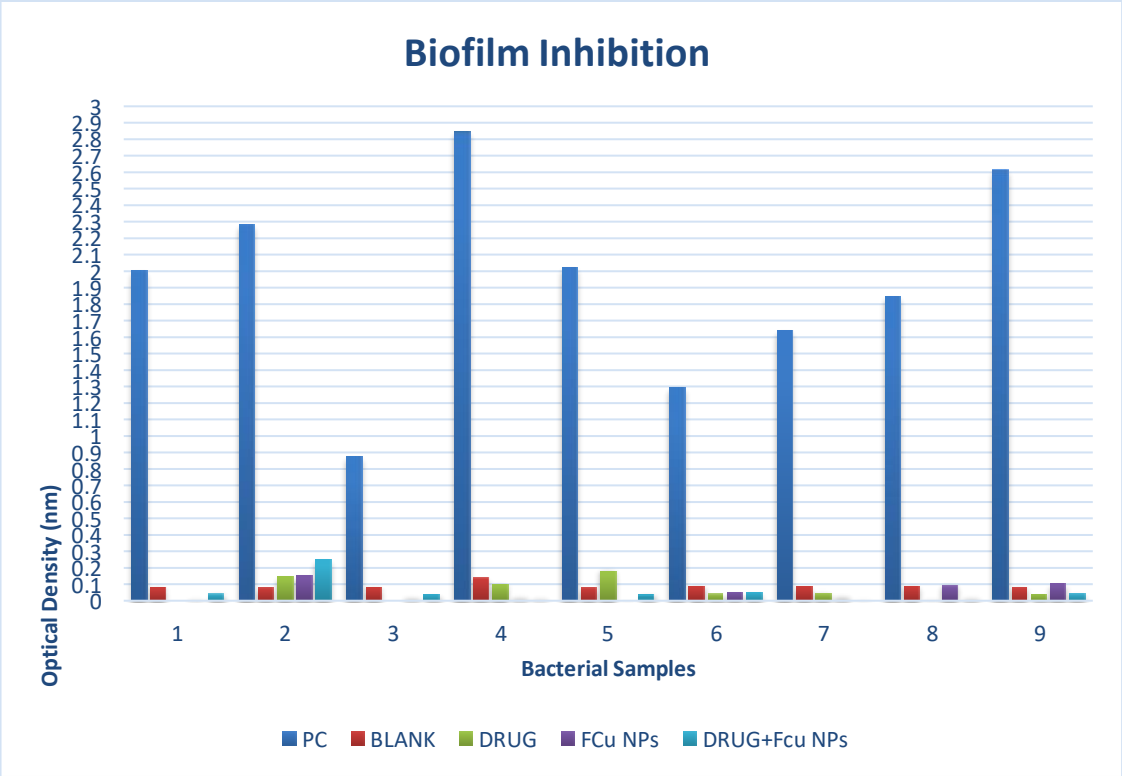

Figure 12: Optical density observed after staining of Biofilm formation and Biofilm inhibition using the conventional drug, FCu Nps alone and synergistically.

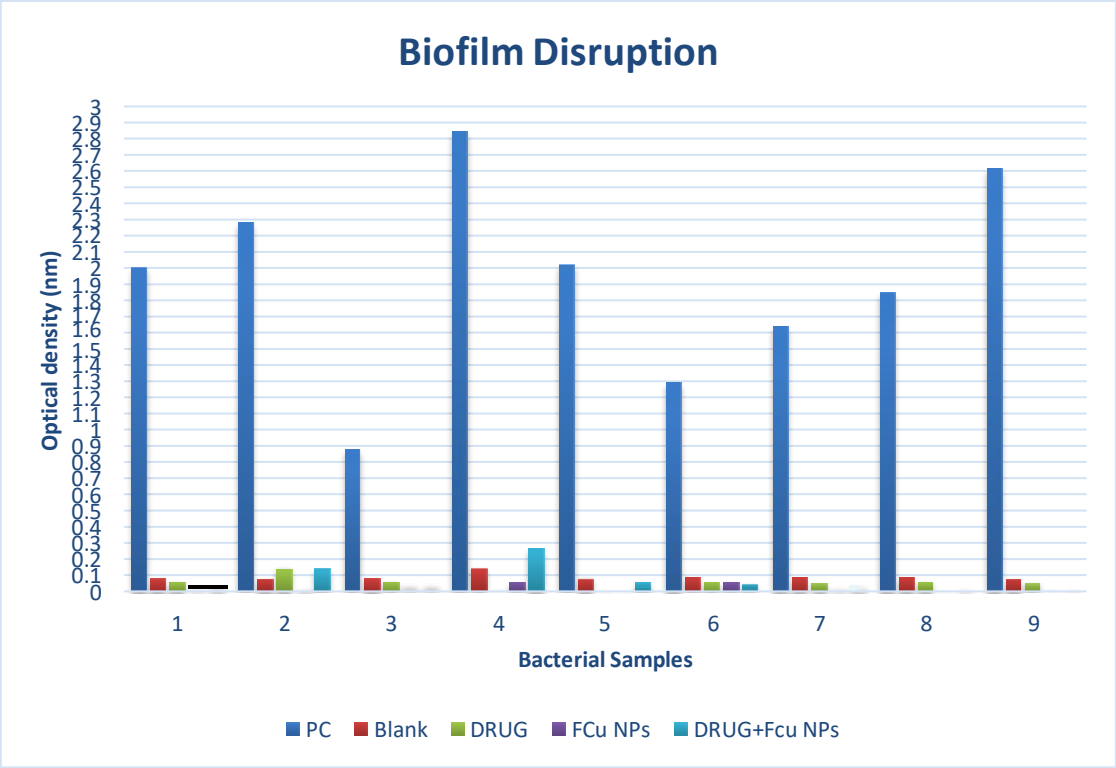

Figure 13: Optical density observed after staining of Biofilm formation and Biofilm disruption using the conventional drug, FCu Nps alone and synergistically.

Table 9: Inhibition Percentage of FCu NPs alone and synergistic with Antibiotic

Disruption of Biofilm in Percentage (%) byFCu Nanoparticles and Drug			
CULTURE CODE	DRUG (I)	FROO2 (I)	FROO2+ DRUG (I)
SIA	93.1	97.9	96.2
SIIA	88.7	97.9	88.4
SIIB	90.4	94.5	94.3
SIIIC1	99.1	96	80.1
SIIIC2a	98.9	99.6	95.2
SVIIB	81.3	80.9	83.2
SIXA	94.9	97.9	96.5
SXIIB	95.3	99.5	98.3
SXIIIC	95.7	98.9	98.6

Table 10: Biofilm Growth Percentage with the Treatment of FCu NPs alone and synergistic with Antibiotic

Biofilm Growth in Wells (%) treated withFCu Nanoparticles and Drug				
CULTURE CODE	Biofilm % in well	DRUG (I)	FROO2 (I)	FROO2+ DRUG (I)
SIA	60.11	4.1	3.39	1.95
SIIA	76.60	3.08	3.48	8.44
SIIB	39.43	10.08	6.86	5.46
SIIIC1	97.03	1.63	4.13	4.35
SIIIC2a	67.10	5.21	3.7	2.07
SVIIB	19.48	3.72	2.99	2.87
SIXA	43.64	2.43	3.43	4.56
SXIIB	67.96	4.26	0.61	3.13
SXIIIC	71.66	1.73	0.94	1.3

Table 11: Disruption Percentage of FCu NPs alone and synergistic with Antibiotic

Inhibition of Biofilm in Percentage (%) byFCu Nanoparticles and Drug			
CULTURE CODE	DRUG (I)	FROO2 (I)	FROO2+ DRUG (I)
SIA	98.4	98.4	94.7
SIIA	87.4	87.4	79.4
SIIB	95.8	95.8	93.6
SIIIC1	98.1	98.1	98.6
SIIIC2a	99.7	99.6	96.6
SVIIB	82.2	82.2	81.6
SIXA	96.9	96.9	98.9
SXIIB	91.2	91.2	97.5
SXIIIC	90.5	90.5	95.7

Table 12: Biofilm Growth Percentage with theTreatment of Fcu NPsalone and synergisticwith Antibiotic

Biofilm Growth in Wells (%) treated withFCu Nanoparticles and Drug				
CULTURE CODE	Biofilm % in well	DRUG (D)	FROO2 (D)	FROO2+ DRUG (D)
SIA	60.11	1.32	3.24	2.56
SIIA	76.60	2.71	2.39	2.88
SIIB	39.43	3.48	6.03	5.94
SIIIC1	97.03	4.57	3.2	4.81
SIIIC2a	67.10	3.36	3.7	1.28
SVIIB	19.48	2.8	2.73	3.22
SIXA	43.64	2.27	4.02	3.21
SXIIB	67.96	1.83	4.32	3.62
SXIIIC	71.66	1.26	2.62	2.49

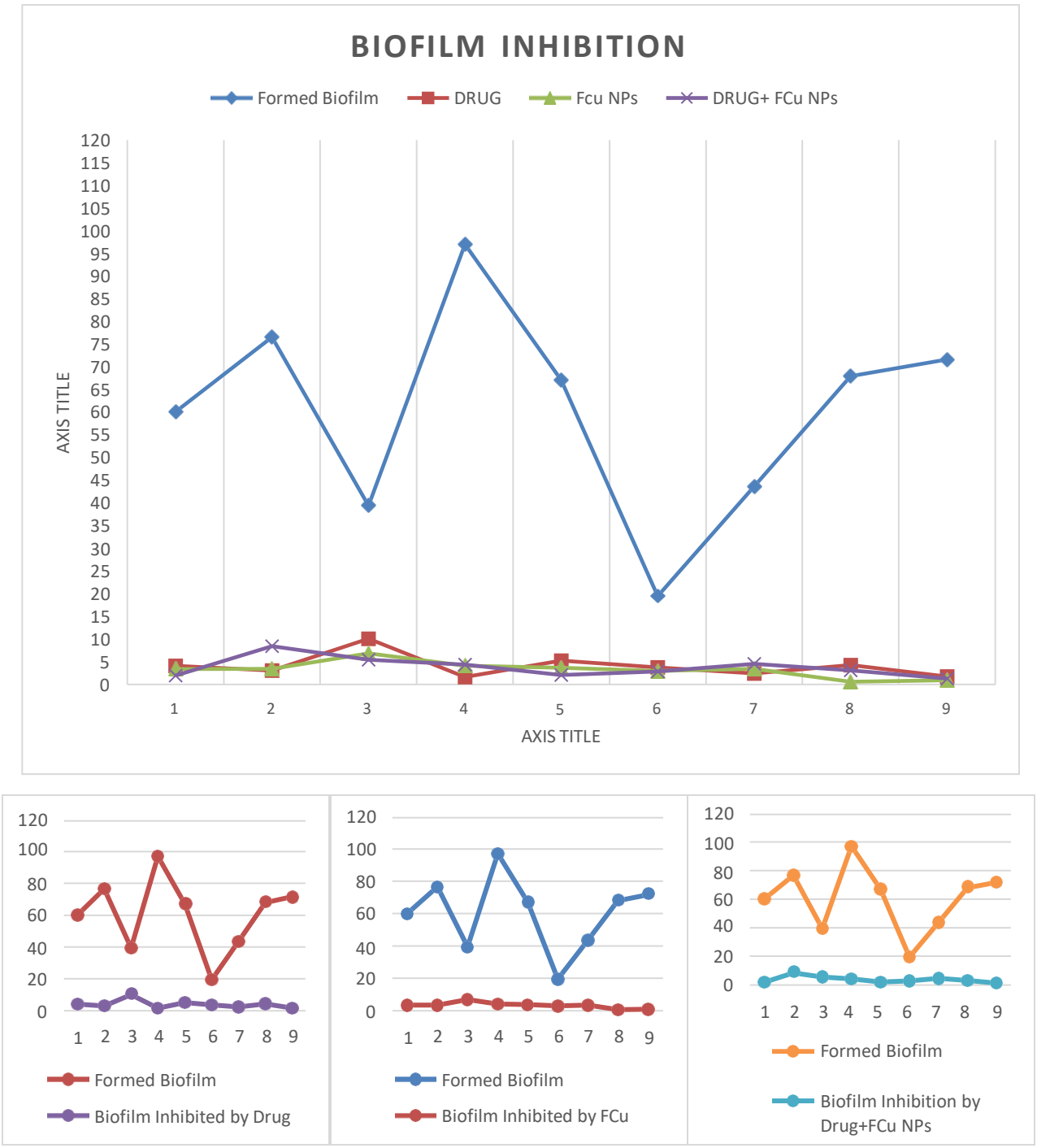

Figure 14: Showing the Percent (%) of biofilm formation and biofilm inhibition. The series shows the drop in the formation of biofilm against the formed biofilm due to the presence of copper nanoparticles (FCu Nps) and the conventional drug alone and synergistically. (for data see Table 9)

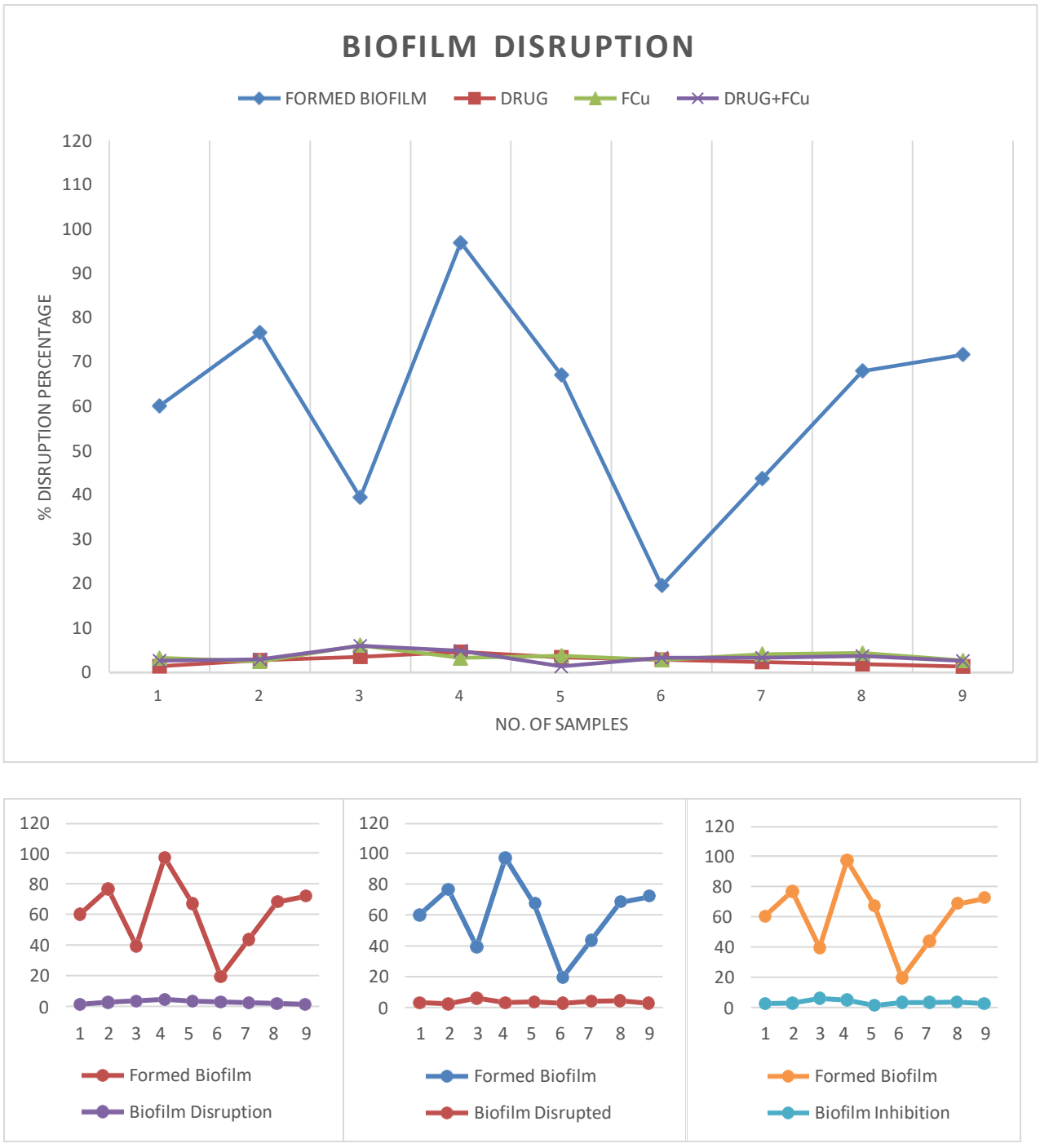

Figure 15: : Showing the Percent (%) of biofilm formation and biofilm disruption. The series shows the disruption in the formed biofilm against the untreated formed biofilm due to the presence of copper nanoparticles (FCu Nps) and the conventional drug alone and synergistically (for data see Table 10)

Discussion

This study shows *Proteus* (SIA and SIIB), *Neisseria* (SIIA), *Pseudomonas* (SIIIC1), to

Corynebacterium (SIIIC2a), *Escherichia* (SVIIB and SIXA), *Klebsiella* (SXIIB) and *Staphylococcus* (SXIIIC) were the bacteria that were isolated from the wound samples are the most prevalent species involved in wound-biofilm formation. The patterns of hemolysis observed confirmed that the strains were pathogenic and can cause secondary infections as well. The nanoparticle synthesised biologically using copper salts and leaves extract of *Ficus religiosa* has more stability, and crystallinity, and has been phytochemically rich (loaded with functional groups). The lattice structure of the particles was in the nano range as determined by P-XRD, with an average particle size of less than 100 nm which concludes the penetrative properties. The antibiofilm and biofilm disruption results have shown their capability to destroy the formed biofilm.

Conclusion

This study reveals that the synthesized Copper nanoparticles from Ficus religiosa leaf extract via the biological route are more stable, crystalline, and least impure loaded with phytochemicals (functional groups). The particles in the nano range have an average particle size between 26-100 nm and the lattice structure is Chalcanthite, triclinic and primitive type as characterised by P-XRD (powder x-ray crystallography). The Isolated bacterial strains from collected wound samples were Staphylococcus sp., Escherichia sp., Klebsiella sp., Proteus sp., Pseudomonas sp., Enterobacter sp., Neisseria sp., Citrobacter sp., Corynebacterium sp., Bacillus sp. All the isolated strains were pathogenic according to the observed patterns of hemolysis and the Anti-microbial and antibiofilm activity of synthesized nanoparticles against the isolated pathogenic microorganisms was found to be significant compared to antibiotics at different concentrations.

Acknowledgement

We wish to express our sincere acknowledgement to Dr. Ashok Kumar Chauhan, President, RBEF parent organization of Amity University Madhya Pradesh (AUMP), Dr. Aseem Chauhan, Additional President, RBEF and chairman of AUMP, Gwalior, Lt. Gen. V.K. Sharma, AVSM (Retd.), Vice Chancellor of AUMP Gwalior, to provide the necessary facilities, valuable support, and encouragement throughout the work.

Conflict of Interest

The authors declare that they have no conflict of interest.

Funding Source

No financial support.

Reference

1. Socransky SS, and Haffajee AD, 2002. Dental biofilms: difficult therapeutic targets. Periodontology 2000,; 28(1), Pages-12-55.
2. Costerton JW, Geesey GG, and Cheng KJ, 1978 How bacteria stick. Scientific America 238(1), Pages- 86-95.
3. Donlan, RM, and Costerton JW, 2022. Biofilms: survival mechanisms of clinically relevant microorganisms. Clinical Microbiology Reviews 15(2), Pages-167-193.
4. James GA, et.al, 2008 Biofilms in chronic wounds. Wound Repair and Regeneration 16(1), Pages-37-44.
5. Bjarnsholt T, et. al. Biofilm infections. Springer New York, eds. 1; 2011.
6. Akiyama H, 1996. Staphylococcus aureus infection on cut wounds in the mouse skin: experimental staphylococcal botryomycosis. Journal of Dermatological Sciences 11(3), Pages-234-238.
7. White R, and Cutting K, 2008. Critical colonisation of chronic wounds: microbial mechanisms. Wounds UK, 2008; 4(1): Pages-70.
8. Akiyama H, et. al, 2003. Assessment of Streptococcus pyogenes microcolony formation in infected skin by confocal laser scanning microscopy. Journal of Dermatological Science 32(3), Pages-193-199.
9. Schaber JA, et. al, 2007. Pseudomonas aeruginosa forms biofilms in acute infection independent of cell-to-cell signaling. Infections and Immunology 75(8), Pages-3715-3721.
10. Davis SC et. al, 2008. Microscopic and physiologic evidence for biofilm-associated wound colonization in vivo. Wound Repair and Regeneration 16(1), Pages- 23-29.
11. Rex JRS, et. al, 2018. Phytochemicals as a potential source for anti-microbial, anti-oxidant and wound healing-a review. MOJ Biorganic and Organic Chemistry 2(2), Pages-

61-70.

12. Hall-Stoodley L, and Stoodley P, 2009. Evolving concepts in biofilm infections. Cellular Microbiology 11(7), Pages-1034-1043.
13. Wolcott RD, et. al, 2010. Chronic wounds and the medical biofilm paradigm. Journal of wound care 19(2), Pages-45-53.
14. Garraud O, Hozzein WN, and Badr G, 2017. Wound healing: time to look for intelligent, 'natural' immunological approaches?. BMC Immunology 18(1), Pages-1-8.
15. Huang Z, et. al, 2008. Toxicological effect of ZnO nanoparticles based on bacteria. Langmuir 24(8), Pages-4140-4144.
16. Morris SA, Farrell D, and Grodzinski P, 2014. Nanotechnologies in cancer treatment and diagnosis. Journal of the National Comprehensive Cancer Network 12(12), Pages-1727-1733.
17. Mazhar T, Shrivastava V, and Tomar RS, 2017 Green synthesis of bimetallic nanoparticles and its applications: a review. Journal of Pharmaceutical Sciences and Research 9(2), Pages-102.
18. Cappuccino JG, and Sherman N, 2008. Microbiology: a laboratory manual. Benjamin-Cummings Publishing Company (Vol. 9).
19. Freeman DJ, Falkiner FR, and Keane CT, 1989. New method for detecting slime production by coagulase-negative staphylococci. Journal of Clinical Pathology 42(8), Pages-872-874.
20. Kaiser TDL, et. al, 2013. Modification of the Congo red agar method to detect biofilm production by Staphylococcus epidermidis. Diagnostic Microbiology and Infectious Disease 75(3), Pages-235-239.
21. Sharma BK, et. al, 2015. Silver inhibits the biofilm formation of Pseudomonas aeruginosa. Advance Microbiology 5(10): Pages-677-85.
22. Sharma D, Kanchi S, Bisetty K, 2019. Biogenic synthesis of nanoparticles: a review. Arabian Journal Chemistry 12(8): Pages-3576-600. doi: 10.1016/j.arabjc.2015.11.002.
23. Panda PS, Chaudhary U, Dube SK. 2016 Comparison of four different methods for detection of biofilm formation by uropathogens. Indian Journal of Pathology and Microbiology 59(2), Pages-177-9. doi: 10.4103/0377-4929.182013, PMID 27166035.
24. Naves P, et. al, 2008. Measurement of biofilm formation by clinical isolates of Escherichia coli is method-dependent. Journal of Applied Microbiology 105(2), Pages-

585-90. doi: 10.1111/j.1365-2672.2008.03791.x, PMID 18363684.

25. Pradhan P, et, al, 2010. Pharmacognostic, phytochemical and quantitative investigation of Saraca asoca leaves. Journal of Pharmaceutical Research 3(4), Pages-776-780.
26. Obafemi TO, et. al, 2017. High-performance liquid chromatography (HPLC) fingerprinting, mineral composition and in vitro antioxidant activity of methanol leaf extract of *Synsepalum dulcificum* (Sapotaceae). Journal of Applied Pharmaceutical Science 7(11), Pages-110-118.
27. Okawa M, et. al, 2001. DPPH (1, 1-diphenyl-2-picrylhydrazyl) radical scavenging activity of flavonoids obtained from some medicinal plants. Biological and Pharmaceutical Bulletin 24(10), Pages-1202-5.
28. Tomar RS, Chauhan PS, and Shrivastava V, 2014. A critical review on nanoparticle synthesis: physicochemical v/s biological approach. World Journal of Pharmaceutical Research 4(1), Pages-595-620.
29. Bindu P, and Thomas S, 2014. Estimation of lattice strain in ZnO nanoparticles: X-ray peak profile analysis. Journal of Theory and Applied Physics 8, Pages-123-34.
30. Sharma R, Bisen DP, and Shukla U, 2012. X-ray diffraction: a powerful method of characterizing nanomaterials. Recent Research in Science and Technology 4(8), Pages-77-79.
31. Shukla N, et. al, 2003. FTIR study of surfactant bonding to FePt nanoparticles. Journal of Magnetism and Magnetic Materials 266(1-2), Pages-178-184.
32. Jaiswal A. K, et. al, 2016. Antimicrobial activity of bimetallic Cu/Pd nanofluids. Journal of Advance Chemistry and Engineering 6(2), Pages-151.
33. Dastjerdi R, and Montazer M, 2010. A review on the application of inorganic nano-structured materials in the modification of textiles: focus on anti-microbial properties. Colloids and surfaces. B: Biointerfaces 79(1), Pages-5-18.
34. Qi L, et. al, 2004. Preparation and antibacterial activity of chitosan nanoparticles. Carbohydrate Research 339(16), Pages-2693-2700.
35. Chamundeeswari M, et. al, 2010. Preparation, characterization and evaluation of a biopolymeric gold nanocomposite with antimicrobial activity. Biotechnology and Applied Biochemistry 55(1), Pages-29-35.
36. Johnston HJ, 2010. A review of the *invivo* and in vitro toxicity of silver and gold particulates: particle attributes and biological mechanisms responsible for the observed

toxicity. Critical Review in Toxicology 40(4), Pages- 328-46.

37. Barapatre A, Aadil KR, and Jha H, 2016. Synergistic antibacterial and antibiofilm activity of silver nanoparticles biosynthesized by lignin-degrading fungus. Bioresources and Bioprocessing 3(1), Pages- 1-13.
38. Haney EF, Trimble MJ, and Hancock RE, 2021. Microtiter plate assays to assess antibiofilm activity against bacteria. Nature Protocols 16(5), Pages-2615-2632.

Eur. Chem. Bull. ***2023****,12(issue 8), 5108-5139*